A Journal of the Gesellschaft Deutscher Chemiker

Angewandte International Edition GDCh Chemie

www.angewandte.org

Accepted Article

Title: Growth of Homogeneous High-density Horizontal SWNT Arrays on Sapphire via a Magnesium-assisted Catalyst Anchoring Strategy

Authors: Jin Zhang, Ying Xie, Liu Qian, Dewu Lin, Yue Yu, and Shanshan Wang

To be cited as: *Angew. Chem. Int. Ed.* 10.1002/anie.202101333

Link to VoR: https://doi.org/10.1002/anie.202101333

WILEY-VCH

10.1002/anie.202101333

WILEY-VCH

COMMUNICATION

Growth of Homogeneous High-density Horizontal SWNT Arrays on Sapphire via a Magnesium-assisted Catalyst Anchoring Strategy

Ying Xie,[a] Liu Qian,[a] Dewu Lin,[a] Yue Yu,[a] Shanshan Wang,[a] Jin Zhang*[a]

[a] Y. Xie,[a] Dr. L. Qian,[a] Dr. D.W. Lin,[a] Y. Yu,[a] Dr. S.S. Wang,[a] Prof. J. Zhang*[a]
Beijing Science and Engineering Center for Nanocarbons, School of Materials Science and Engineering, College of Chemistry and Molecular Engineering
Peking University, Beijing 100871, P. R. China.
E-mail: jinzhang@pku.edu.cn

Supporting information for this article is given via a link at the end of the document.

Abstract: *In-situ* growth of high-density single-walled carbon nanotube (SWNT) arrays with homogeneity is highly desirable for integrated circuits. However, disastrous migration and aggregation of catalyst nanoparticles on substrate has greatly limited the area of as-grown SWNT arrays. Herein, we develop a magnesium-assisted catalyst anchoring strategy to restrain catalyst nanoparticles sintering on substrate. Magnesium modification ameliorates sapphire surface by high temperature solid reaction and thus provides a stronger metal-support interaction (SMSI). Hereby, we realize the direct growth of high-density SWNT arrays that fully cover an entire 10×10 mm^2 substrate with the local highest density of ~110 tubes μm^{-1} using iron as catalyst. This strategy was also proven universal when employing solid carbide catalysts.

Decades have witnessed the rapid development of carbon nanotubes (CNTs), which have been put on a very high pedestal in digital logic technology. The superior electrical properties of single-walled carbon nanotube (SWNT), especially the high-density horizontal SWNT arrays, make it an ideal candidate for the channel in a scaled-down transistor. During the past few decades, several methods have been developed for high-density horizontal SWNT arrays fabrication. For post-processing, gold film assisted transfer of CNTs implemented a wafer-scale massive aligned nanotubes on 4 inch Si/SiO_2 wafers.[1] Classic Langmuir–Blodgett[2] and Langmuir–Schaefer[3] methods have been utilized to obtain SWNT arrays with ultra-high density of 500 tubes μm^{-1}. Recently, Peng's group also developed a multiple dispersion and sorting process making CNT arrays with a tunable density of 100 to 200 tubes μm^{-1} on a 10-centimeter silicon wafer.[4] Although post-processing can realize SWNT arrays with super large-area coverage or high-density, the inevitable use of polymers and multiple dispersion may degrade SWNT arrays' quality and arrangement. Most importantly, this processing vastly increases the cost as well. Therefore, direct growth is desirable to solve all these problems. For *in-situ* growth, methods of patterning $CuCl_2$/polyvinylpyrrolidone (PVP) alcohol solution on quartz,[5] multiple loading catalysts,[6] multiple-cycle chemical vapor deposition (CVD) method,[7] periodic approach[8] and multi-cycle *in-situ* loading catalysts[9] all realized CNT arrays with density of 10-70 tubes μm^{-1}. However, it is still far beyond the requirement for achieving 100-200 tubes μm^{-1} in CNT-based integrated circuits. In this regards, our previous work has reported a catalyst-dissolving and -releasing process named Trojan catalyst and an improved Trojan-Mo catalyst, successfully increasing the highest density of SWNT arrays to 130-160 tubes μm^{-1}.[10] Nevertheless, some of the released Trojan catalysts still tended to migrate and aggregate, which restricted the area of SWNT arrays in the range of several hundred microns, severely limiting their use in large-scale device integration. Hence, fabricating wafer-scale high-density SWNT arrays in low cost is highly desired for high-performance integrated circuits based on CNTs.

With the aim to inhibit catalyst aggregation on flat substrates during CVD process, the surface structure of the substrate itself cannot be ignored. In heterogeneous catalysis, the selection of a suitable support with necessary structural and morphological modulation is an effective approach to improve the activity and eliminate the sintering of active metals loaded on it. For instance, magnesium-modified alumina support has been proved effective to maintain a highly dispersion of metal particles by offering a strong metal−support interaction (SMSI).[11] Furthermore, the SMSI effect also makes metal ions more difficult to be reduced and can obtain lower metal particle size. Therefore, to entail SMSI effect thus eliminate aggregation, introducing magnesium into sapphire can be at play. Herein, we develop a universal strategy to optimize the interaction between catalyst and substrate by designing a novel magnesium-modified sapphire surface. Through high temperature solid reaction of magnesium salt and sapphire surface during annealing, magnesium incorporation into alumina lattice occurs and the catalyst metal particles, either exsolved from the lattice or directly loaded on the surface, can exhibit an increasing robustness and a highly uniform dispersion. With this design, we successfully prepare the homogeneous high-density horizontal SWNT arrays on an entire 10×10 mm^2 sapphire substrate.

To modify substrate surface, magnesium and iron precursors were spin-coated on sapphire, followed by an annealing process (Figure 1a). After CVD growth, the sapphire wafer (10×10 mm^2) was fully covered with high-density horizontal SWNT arrays. In scanning electron microscope (SEM), Figure 1c, we selected five different areas on one substrate to zoom in and the observations demonstrated the homogeneity of the as-grown SWNT arrays. Atomic force microscope (AFM) image further indicated the highest density of SWNT arrays to be as high as ~110 tubes μm^{-1} (Figure 1b), which meets the requirement of 100~200 tubes μm^{-1} for CNT applications in nano-electronics. More SEM and AFM images in Figure S1 indicated the density of 60 tubes μm^{-1} for the entire substrate can be guaranteed. Line-scanning Raman spectra of SWNT arrays excited by 532 nm laser with scarcely any D bands testified the high quality of SWNT arrays.

10.1002/anie.202101333
WILEY-VCH

COMMUNICATION

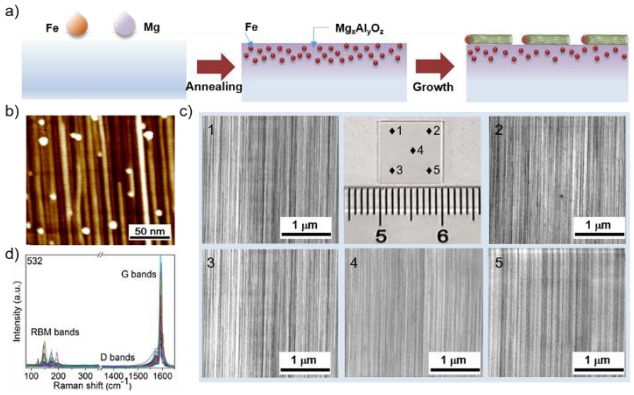

Figure 1. Characterization of homogeneous high-density SWNT arrays a) Preparation process; b) AFM image exhibited the local density of SWNT arrays can be as high as ~110 tubes μm^{-1}; c) SEM images chosen from five different areas on one sapphire substrate demonstrated the homogeneity; d) Line-scanning Raman spectra of SWNT arrays with 532 nm excitation (Scanning step: 5 μm).

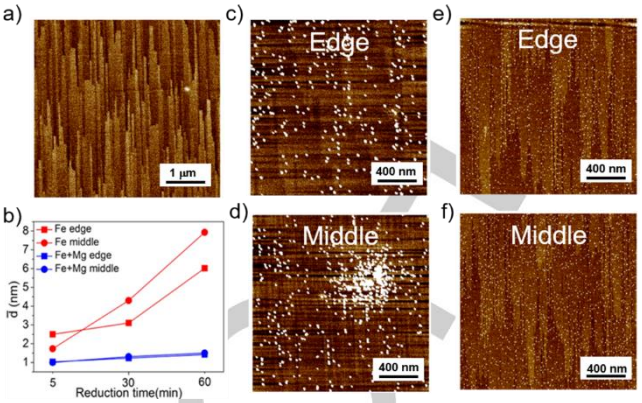

Figure 2. Size and distribution of nanoparticles a) AFM image of sapphire loaded with iron and magnesium after annealing; b) Statistics of the average diameters of nanoparticles with respect to H_2 reduction time (5 min, 30 min and 1h) in a given area (2 μm × 2 μm). The error bars for the average diameters are standard deviations; AFM images of catalyst nanoparticles from the edge and middle of the sapphire substrate c-d) loaded with iron alone and e-f) loaded with both iron and magnesium.

Homogeneous growth of high-density SWNT arrays owes to highly active catalyst nanoparticles, which are sinter-resistant thus highly dispersed on the entire substrate during CVD. AFM image shown in Figure 2a indicated the as-annealed substrate loaded with magnesium and iron precursors remained almost the same morphology as pure sapphire and no nanoparticles formed on it, in accordance with impregnation and exsolution mechanism of Fe^{3+} on alumina.[10, 11c, 11d] Besides, magnesium also 'disappeared' on sapphire surface, which will be elaborated in the next section. Here, to compare migration and aggregation of nanoparticles on sapphire with different processing, reduction by H_2 for different time has been carried out. Figure 2b compiled the data for average diameters of nanoparticles formed after H_2 reduction with respect to reduction time. Four groups of data were selected from a given area (2 μm × 2 μm) on the edge (marked with square) and in the middle (marked with circle) of the substrate loaded with iron alone and with iron plus magnesium, as indicated in the figure by the red line and blue line, respectively. From Figure 2b we can learn that nanoparticles exsolved from sapphire loaded with both magnesium and iron exhibited an overall smaller size and narrower diameter distribution. Furthermore, those nanoparticles showed an incredible robustness against sintering thus a highly uniform dispersion as H_2 reduction time went on. Especially after 1h H_2 treatment, the difference was very significant. As shown in Figure 2c and 2d, without the participation of magnesium, nanoparticles migrated and aggregated disastrously on sapphire surface, particularly in the middle of it. On the contrary, nanoparticles grown on sapphire loaded with magnesium and iron were highly sinter-resistant, exhibiting basically the same average diameter and distribution, see Figure 2e and 2f. Other AFM images and histogram of nanoparticles in H_2 treatment were displayed in Figure S2-S4. All of these results implied an indispensable role of magnesium for the fabrication of homogeneous high-density SWNT arrays.

In order to unravel the effect of magnesium, more characterization methods are requisite. Firstly, we conducted X-ray photoelectron spectroscopy (XPS), which confirmed the existence of both iron and magnesium on the as-annealed sapphire (Figure 3a, 3b and S5). In addition, contrasting XPS spectral of iron on sapphire loaded with both iron and magnesium with that on pure sapphire, we discovered a slight increase in binding energy of Fe 2p. It has been reported that the increase in binding energy can be attributed to the size effect, that is, binding energy increases when nanoparticle size decreases.[12] It is also possible there is a charge transfer between nanoparticles and the support, which induces SMSI to anchor nanoparticles. All of these conjectures are in line with what has been concluded from H_2 reduction treatment in Figure 2. Besides, as alluded in Figure 2a, not only iron but also magnesium 'disappeared' from the substrate after annealing. Combining AFM with XPS results, we tentatively assumed that both iron and magnesium are able to embed into alumina lattice and store in sub-surface during high temperature processing instead of being volatilized, which is in compliance with literatures of solid reaction among magnesium, iron and alumina to form diverse spinel-like structure on sapphire surface as mentioned above. To verify this speculation, we further implemented XPS depth profiling by removing the surface layer by layer with argon bombardment. The result (Figure 3c) consolidated the content of both iron and magnesium decreased with the increase of analyzed depth. Moreover, most of iron and magnesium concentrated in shallow sub-surface of sapphire. During CVD growth, catalyst nanoparticles exsolved from alumina lattice in reducing atmosphere, as confirmed by H_2 reduction treatment in Figure 2. High-resolution transmission electron microscopy (HRTEM) was applied to identify the detailed roles of iron and magnesium. As shown in Figure 3d, an individual SWNT was connected to a nanoparticle, which involved two different grains. Figure 3e showed the fast Fourier transform (FFT) images corresponding to the two grains, respectively. Careful crystallographic analysis indicated that both two grains can be assigned to γ-Fe_2O_3 but were imaged along different zone axes. The lattice plane indexes corresponding to each reflection spots, as well as the interplanar spacings calculated in light of the

10.1002/anie.202101333

distances measured in the reciprocal space, were all clearly marked, which were well consistent with the lattice parameters of γ-Fe_2O_3. The left panel of Figure 3e showed the atomic model of γ-Fe_2O_3 with brown and red spheres representing Fe and O atoms, respectively. The simulated diffraction pattern of γ-Fe_2O_3 along the zone axis of <332> was displayed in the right panel of Figure 3f, which agreed perfectly with the FFT pattern at the bottom panel of Figure 3e, further verifying our deduction of the nanoparticle composition and structure. The formation of ferric oxide might be derived from the oxidation of the catalyst iron nanoparticles during the TEM sample preparation, which involved baking and annealing in ambient conditions. It is worth noting that no magnesium nanoparticles were detected on SWNTs. In addition, a larger-scale energy dispersive X-ray spectroscopy (EDS) spectrum (Figure 3g) of the TEM specimen also showed no magnesium signal, manifesting again the absence of magnesium nanoparticles precipitated from the substrate surface. EDS mapping images were displayed in Figure S6. This is not surprising since magnesium entered into alumina lattice by annealing, which, then, cannot be dragged out of the substrate lattice by H_2 reduction, thus reserved in the sub-surface of sapphire. Hereto, as indicated in Figure 3h, we speculate that the mechanism of preparing homogeneous high-density SWNT arrays that fully covered the entire sapphire is the construction of a brand-new sapphire surface by magnesium modification. During annealing, magnesium enters into alumina lattice and produces, perhaps, magnesium aluminate on the surface, which ameliorates properties of the sapphire surface. The new surface accordingly exhibits a significant advantage over pure sapphire in terms of restraining the sintering of exsolved iron nanoparticles by providing a SMSI effect. The homogenous distribution of iron nanoparticles with smaller diameter therefore holds accountable for the growth of high-density horizontal SWNT arrays with homogeneity.

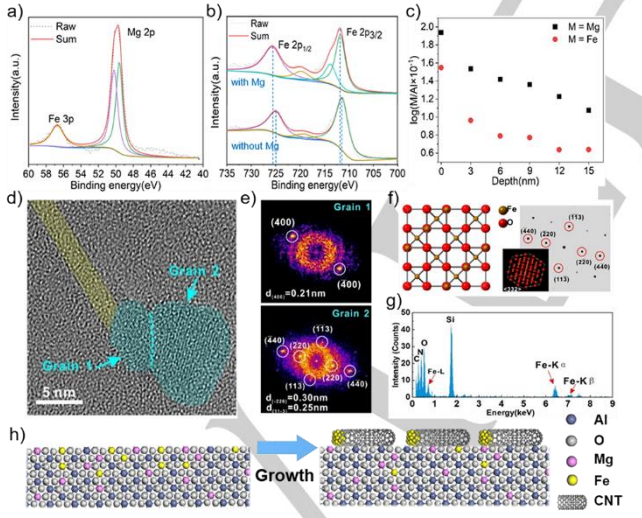

Figure 3. a-b) XPS spectra confirmed the existence of magnesium and iron on sapphire substrate; c) XPS depth analysis after annealing; d) HRTEM image of an individual SWNT connected to two catalyst particles; e) the corresponding FFT pattern; f) Atomic model and simulated diffraction pattern proved both particles to be ferric oxide; g) A larger-scale EDS spectrum shows that there is no magnesium signal; h) Schematic illustration of SWNT arrays growth mechanism on magnesium-modified sapphire with iron catalyst.

As stated above, the desirable growth of homogeneous high-density horizontal SWNT arrays resorts to the magnesium-modified sapphire surface, which ameliorates SMSI thus endows nanoparticles grown on it a robust sinter-resistance. Based on this assumption, we speculate that this design might not be restricted in iron catalyst. Similarly, other catalyst nanoparticles might highly disperse on this new surface as well. In structural controlled growth of SWNTs, solid carbide catalysts, such as Mo_2C and WC, are always applied due to retainment of its crystalline structure in high temperature.[13] Therefore, we also apply these carbide catalysts to verify the universality of the magnesium-assisted catalyst anchoring strategy. The preparation process was (Figure 4a) dispersing catalyst precursor containing molybdenum or tungsten on the as-annealed magnesium-modified sapphire. After carbonization, Mo_2C or WC was obtained *in-situ* to grow SWNT arrays with specific structure. SEM images in Figure 4b and 4c affirmed the homogeneous growth of SWNT arrays with the average density of 20 to 30 tubes μm^{-1}. Line-scanning Raman spectral with 633 nm excitation (Figure 4d and 4e) indicated an enrichment tendency for specific chirality of SWNT. The bands around 1400 cm^{-1} stemmed from sapphire itself with 633 nm excitation.

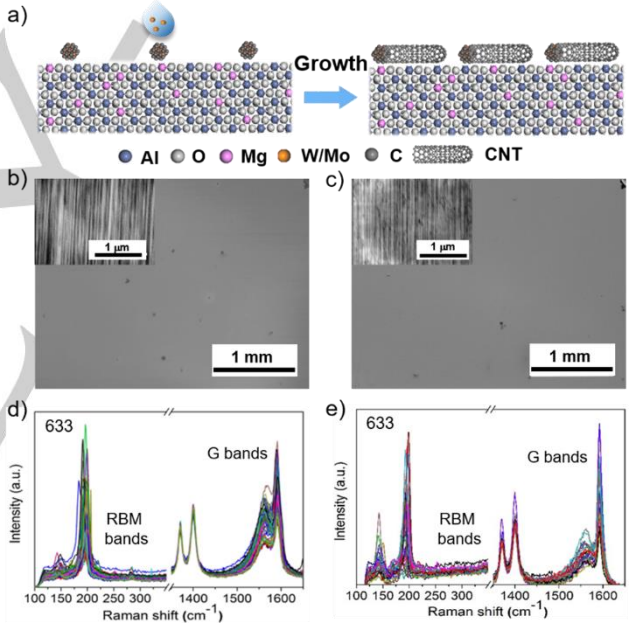

Figure 4. a) Schematic illustration of SWNT arrays growth mechanism with carbide catalysts on magnesium-modified sapphire; SEM images of b) Mo_2C and c) WC catalyzed homogeneous high-density SWNT arrays (inset: zoom-in SEM images); Corresponding line-scanning Raman spectra (633 nm excitation) of SWNT arrays on magnesium-modified sapphire with d) Mo_2C and e) WC as catalyst.

With the assistance of magnesium-modified sapphire, we obtained highly dispersed catalyst nanoparticles thus successfully fabricated the homogeneous high-density SWNT arrays. However, to further scale-up the sample size, the interaction model of airflow and substrate is certain to exert a fairly dramatic effect on homogeneity of SWNT arrays. When combining substrate modification strategy with a redesigned spraying chemical vapor deposition system, the fabrication of wafer-scale homogenous high-density SWNT arrays is believed to come true in the near future.

In summary, we develop a universal magnesium-assisted catalyst anchoring strategy of growing homogeneous high-density SWNT arrays. With iron as catalyst, we realized the growth of SWNT arrays with the highest density of ~110 tubes μm^{-1} on a 10×10 mm^2 sapphire. This strategy was also universal to obtain high-density SWNT arrays when using Mo_2C or WC as catalyst. Further combing substrate modification, catalyst design and a spraying chemical vapour deposition system, growth of high-density SWNT arrays that fully cover the wafer-scale substrate with controlled structure will stand a good chance in the near future, which provides a feasible way to solve bottleneck problems and urges SWNT from the laboratorial stage to the real applications.

Acknowledgements

This work was financially supported by the Ministry of Science and Technology of China (2016YFA0200100 and 2018YFA0703502), the National Natural Science Foundation of China (Grant Nos. 52021006, 51720105003, 21790052, 21974004), the Strategic Priority Research Program of CAS (XDB36030100), and the Beijing National Laboratory for Molecular Sciences (BNLMS-CXTD-202001).

Keywords: single-walled carbon nanotube arrays • high-density • homogeneous • sapphire • magnesium-modification

[1] K. Ryu, A. Badmaev, C. Wang, A. Lin, N. Patil, L. Gomez, A. Kumar, S. Mitra, H. S. P. Wong, C. W. Zhou, *Nano Lett.* **2009**, *9*, 189-197.

[2] X. L. Li, L. Zhang, X. R. Wang, I. Shimoyama, X. M. Sun, W. S. Seo, H. J. Dai, *J. Am. Chem. Soc.* **2007**, *129*, 4890-4891.

[3] Q. Cao, S. J. Han, G. S. Tulevski, Y. Zhu, D. D. Lu, W. Haensch, *Nat. Nanotechnol.* **2013**, *8*, 180-186.

[4] L. J. Liu, J. Han, L. Xu, J. S. Zhou, C. Y. Zhao, S. J. Ding, H. W. Shi, M. M. Xiao, L. Ding, Z. Ma, C. H. Jin, Z. Y. Zhang, L. M. Peng, *Science* **2020**, *368*, 850-856.

[5] L. Ding, D. N. Yuan, J. Liu, *J. Am. Chem. Soc.* **2008**, *130*, 5428-5429.

[6] S. W. Hong, T. Banks, J. A. Rogers, *Adv. Mater.* **2010**, *22*, 1826-1830.

[7] W. W. Zhou, L. Ding, S. Yang, J. Liu, *ACS Nano* **2011**, *5*, 3849-3857.

[8] B. Wu, D. C. Geng, Y. L. Guo, L. P. Huang, J. Y. Chen, Y. Z. Xue, G. Yu, Y. Q. Liu, H. Kajiura, Y. M. Li, *Nano Res.* **2011**, *4*, 931-937.

[9] W. M. Liu, S. C. Zhang, L. Qian, D. W. Lin, J. Zhang, *Carbon* **2020**, *157*, 164-168.

[10] aY. Hu, L. X. Kang, Q. C. Zhao, H. Zhong, S. C. Zhang, L. W. Yang, Z. Q. Wang, J. J. Lin, Q. W. Li, Z. Y. Zhang, L. M. Peng, Z. F. Liu, J. Zhang, *Nat. Commun.* **2015**, *6*; bL. X. Kang, Y. Hu, H. Zhong, J. Si, S. C. Zhang, Q. C. Zhao, J. J. Lin, Q. W. Li, Z. Y. Zhang, L. M. Peng, J. Zhang, *Nano Res.* **2015**, *8*, 3694-3703.

[11] aD. N. Bangala, N. Abatzoglou, E. Chornet, *Aiche J.* **1998**, *44*, 927-936; bE. Cho, Y. H. Lee, H. Kim, E. J. Jang, J. H. Kwak, K. Lee, C. H. Ko, W. L. Yoon, *App.l Catal. A-Gen* **2020**, *602*; cS. A. Theofanidis, V. V. Galvita, H. Poelman, N. V. R. A. Dharanipragada, A. Longo, M. Meledina, G. Van Tendeloo, C. Detavernier, G. B. Marin, *ACS Catal.* **2018**, *8*, 5983-5995; dN. V. R. A. Dharanipragada, L. C. Buelens, H. Poelman, E. De Grave, V. V. Galvita, G. B. Marin, *J. Mater. Chem. A* **2015**, *3*, 16251-16262.

[12] J. Ashok, S. Kawi, *ACS Catal.* **2014**, *4*, 289-301.

[13] aS. C. Zhang, L. M. Tong, Y. Hu, L. X. Kang, J. Zhang, *J. Am. Chem. Soc.* **2015**, *137*, 8904-8907; bS. C. Zhang, L. X. Kang, X. Wang, L. M. Tong, L. W. Yang, Z. Q. Wang, K. Qi, S. B. Deng, Q. W. Li, X. D. Bai, F. Ding, J. Zhang, *Nature* **2017**, *543*, 234-238.

10.1002/anie.202101333

WILEY-VCH

COMMUNICATION

Entry for the Table of Contents

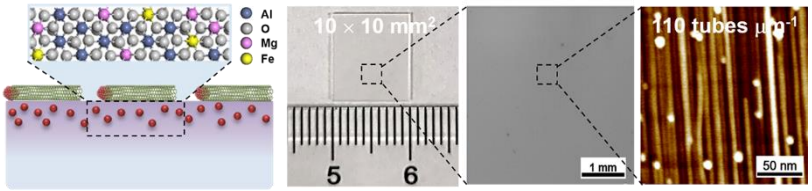

A magnesium-modification strategy was developed for anchoring catalyst nanoparticles on sapphire. The modified sapphire outperformed the pure one by offering a stronger metal-support interaction (SMSI). By virtue of this, we successfully realized the homogeneous single-walled carbon nanotube (SWNT) arrays with the highest density of 110 tubes μm^{-1}. When combined with a spraying chemical vapour deposition and catalyst design, growing homogeneous high-density SWNT arrays in wafer-scale with controlled structure will stand a good chance in the near future.